dCORSIKA update

Dmitry Chirkin
chirkin@physics.berkeley.edu

University of California at Berkeley, USA

Abstract

Release 6.016 of CORSIKA contains an important update that has improved the curved atmosphere treatment. In addition, surface of the Earth can now be considered curved by the internal AMANDA release (dCORSIKA). It is shown that the unphysical sharp suppression of the muon flux at zenith angles close to 90° (just above or below the horizon), previously caused by code constraints, is now non-existent. This makes the current CORSIKA release applicable for muon analyses for which shallow angles are important (e.g. UHE muon background evaluation). In addition, a detailed account is presented and recommendations are given for all speed/size optimization and other settings for use with AMANDA Monte-Carlo chain (mass production).

dCORSIKA code homepage is
http://area51.berkeley.edu/~dima/work/CORSIKA/

1 Introduction

It was previously shown [1] that the Berkeley implementation of CORSIKA for AMANDA exhibits an unexpected suppression in the number of muons coming from angles near the horizon. For the angles affected (above 88°) the distance a muon has to travel through ice to reach the detector is 45.0 km (or 48.7 km for flat surface geometry). As is shown below, less than 0.1% of muons with energies as high as 26.6 PeV can penetrate through this much ice. From [2] the typical energy of a muon that travels this far is $1.5 \cdot 10^{20}$ eV. For the angle at which a 10% reduction was observed (88.9°) these numbers are even higher: the distance to the surface is 70.1 km (90.1 km for flat surface geometry) and the energy at which less than 0.1% of muons penetrate through this distance is 8.6 EeV, the typical energy being $7.54 \cdot 10^{26}$ eV. Therefore the suppression of the muon flux observed from angles near the horizon is believed to be unimportant for the typical AMANDA analyses. However, some analyses (e.g. UHE) consider muons with energies up to 10^{20} eV and the observed suppression could alter their result.

In [1] several possible reasons were given for the muon flux suppression effect. Among them were higher muon decay and energy loss at the horizon, possible magnetic field influence, and the effect of particles with zenith angles greater than 90° being cut throughout the CORSIKA code.

A 400 GeV muon has a free path of 2500 km, and is on average produced at an altitude of 24 km or higher for larger zenith angles. A horizontal muon travels more than 550 km before entering the ice. It has at least a 20% chance of decaying before entering the detector. This probability depends exponentially on the traveled distance and grows fast for zenith angles approaching 90°. So a small reduction of the muon flux at the horizon is to be expected.

The muon energy loss is proportional to the mass overburden of air it crossed. This mass overburden grows from 7 mwe (at the South Pole) for the vertical muon track to 149 mwe for the horizontal track. A 400 GeV muon traveling to the surface loses on average 2.8 GeV for the vertical track and 60 GeV for the horizontal track. If a constant muon energy threshold is maintained for all zenith angles, then more muons from higher zenith angles arrive at the observation point with energies below the threshold. For the muon energy distribution with spectral index 2.7 to 3.7 the reduction of integrated muon flux for $\theta = 0^\circ$ is 1.2% to 1.9%, while for $\theta = 90^\circ$ this reduction is 21% to 31%. Clearly, this further reduces the number of horizontal muon tracks, while leaving the number of vertical muon tracks almost unchanged.

Magnetic field influence is less obvious and probably less prominent. To a certain extent its effect is demonstrated throughout this report. As for the cuts on particles with zenith angles greater than 90°, made in many places inside the CORSIKA code, their effect is greatly reduced when one uses the detector (rather than surface) frame of reference and considers Earth's surface to be curved. Angles less than 90° in the detector frame are mapped into angles below 88.9° in the surface (CORSIKA) frame, where the current version of CORSIKA demonstrates almost no reduction caused by code constraints. The situation is much improved compared to the previous version (6.015) with which it was impossible to completely get rid of the sharp muon reduction at 90° even in the detector frame.

2 Zenith angle distributions

The latest CORSIKA update (ver. 6.016) improves the range estimation of particles in the curved version to get a correct arrival point even below the observation level. Particles below the detector plane are now brought to the output [3]. The improvement in the zenith angle distribution generated with CORSIKA version 6.016 as compared to 6.015 is shown in Fig. $1-2$. The suppression of muons

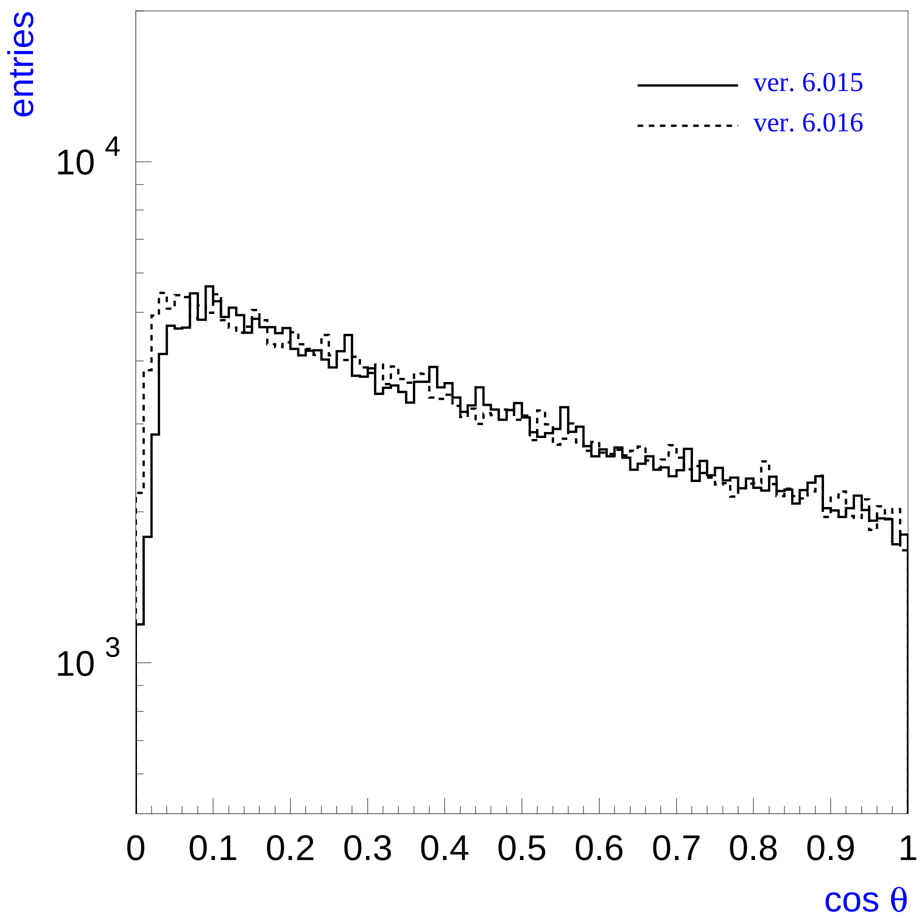

Fig. 1: improvement of zenith angle distributions

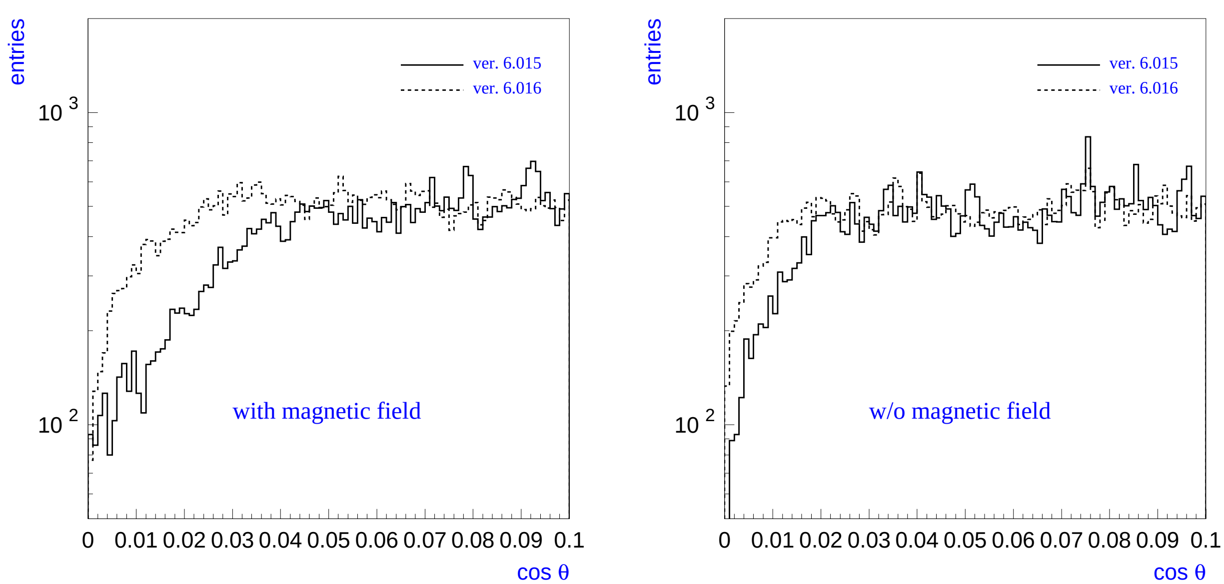

Fig. 2: zenith angle distributions near the horizon

coming from near the horizon is clearly smaller in CORSIKA 6.016. The magnetic field exacerbates this suppression in both old and new CORSIKA versions.

Next, the CORSIKA frame of reference is mapped into the detector frame. This is not necessary if the surface of the Earth can be considered flat. However, in addition to making the treatment more precise, it allows to map the good CORSIKA region that exhibits no suppression ($0°$ to $88.67°$) into the whole range of zenith angles from $0°$ to $90°$ in the detector frame (Fig. 3):

$$\sin\theta_c = \sin\theta_d(1 - h/R)$$

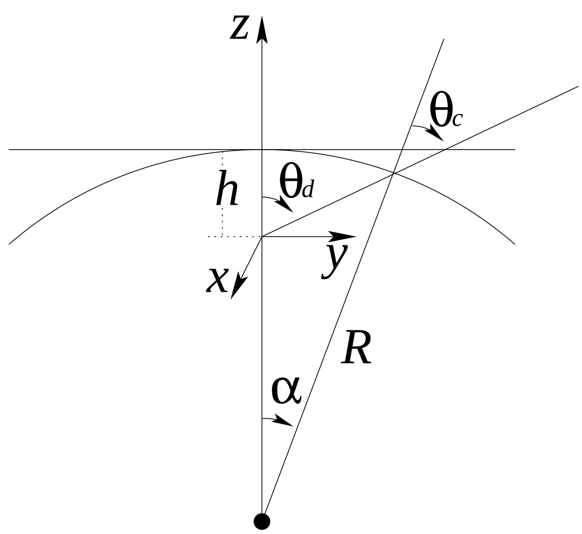

Fig. 3: CORSIKA (θ_c) to detector (θ_d) angle mapping

All shower coordinates and angles are transferred from the CORSIKA (c) frame of reference to the detector (d). To ensure that the magnetic field direction is described as well as possible, the CORSIKA frame is chosen so as to match the detector frame by one rotation by α, performed around the center of the Earth. The coordinate transformation between the two frames can be written as

$$\left\|\begin{matrix} x_d \\ y_d \\ z_d \end{matrix}\right\| = A \cdot \left[\begin{pmatrix} \cos\alpha\cos\phi & \cos\alpha\sin\phi & \sin\alpha \\ -\sin\phi & \cos\phi & 0 \\ -\sin\alpha\cos\phi & -\sin\alpha\sin\phi & \cos\alpha \end{pmatrix} \cdot A^T \left\|\begin{matrix} x_c \\ y_c \\ z_c \end{matrix}\right\| + \left\|\begin{matrix} R\sin\alpha \\ 0 \\ R(\cos\alpha - 1) \end{matrix}\right\| \right]$$

$$\text{with} \quad A = \begin{pmatrix} \cos\phi & -\sin\phi & 0 \\ \sin\phi & \cos\phi & 0 \\ 0 & 0 & 1 \end{pmatrix}$$

Here ϕ is the azimuth angle of the primary. x_c, y_c are randomized inside the projection of the cylinder of the detector on the surface of the Earth made along the direction of the primary. CORSIKA coordinates (x_c, y_c, z_c) are given inside the plane tangent to the surface of the Earth at an intersection point of the shower core with the surface, therefore $z_c = 0$. Once in the detector frame, all particles are propagated from the tangent plane to the surface of the Earth. A similar transformation was applied to the angles at which particles enter the surface. The change in the magnetic field direction introduced by this transformation is given by the rotation angle α, the maximum value of α in the upper hemisphere being $1.3°$.

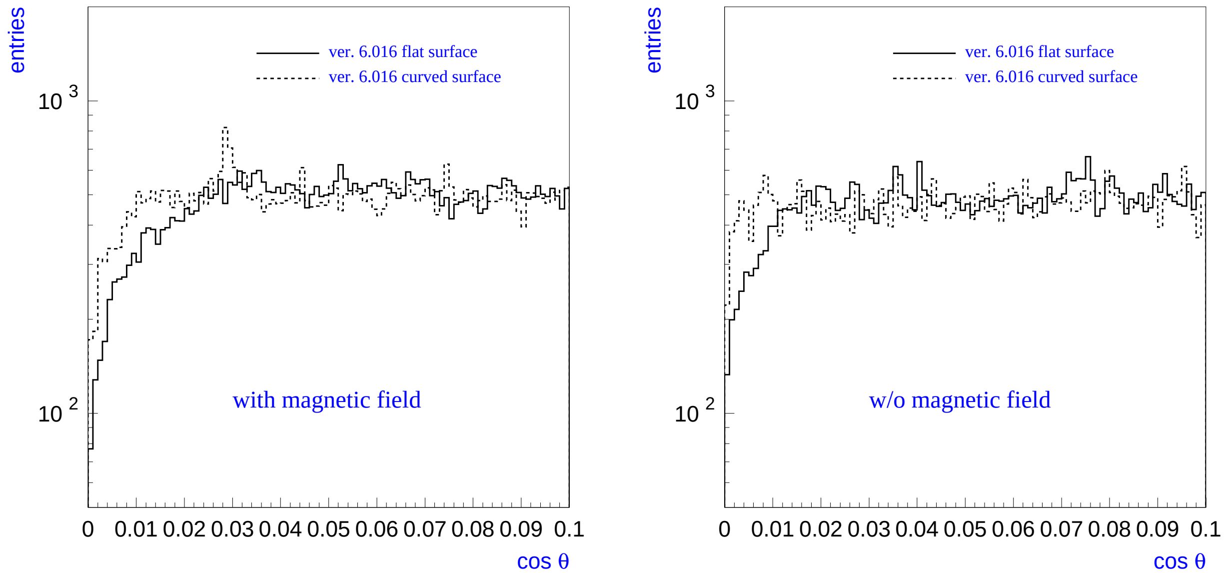

Fig. 4: comparison of flat with the curved surface of the Earth models

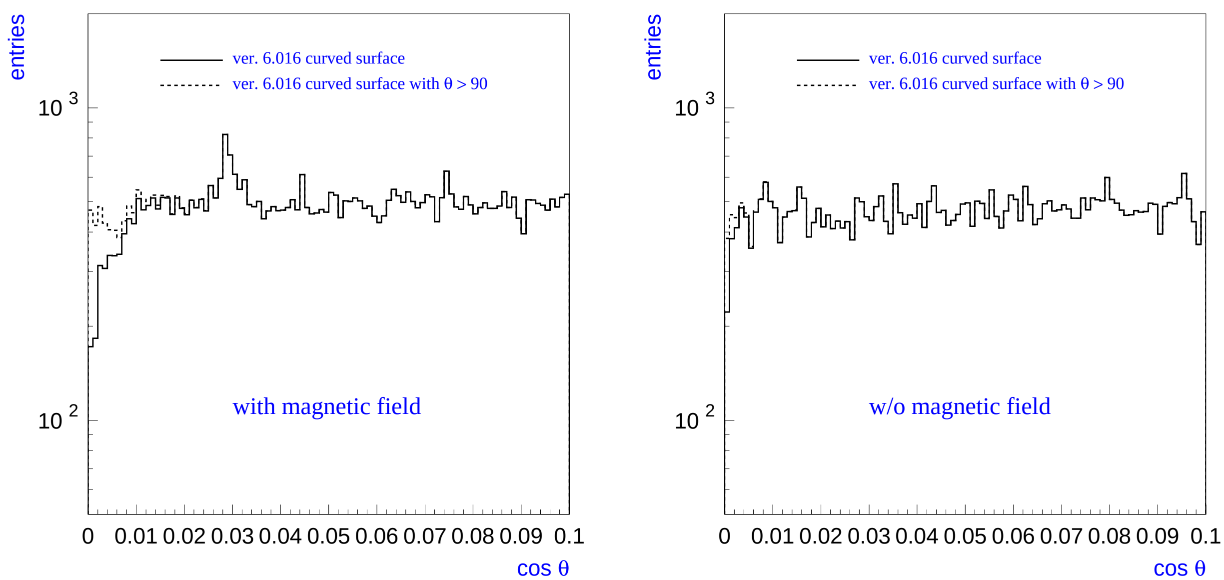

Fig. 5: adding events coming from below the horizon fills the lowest angle bins

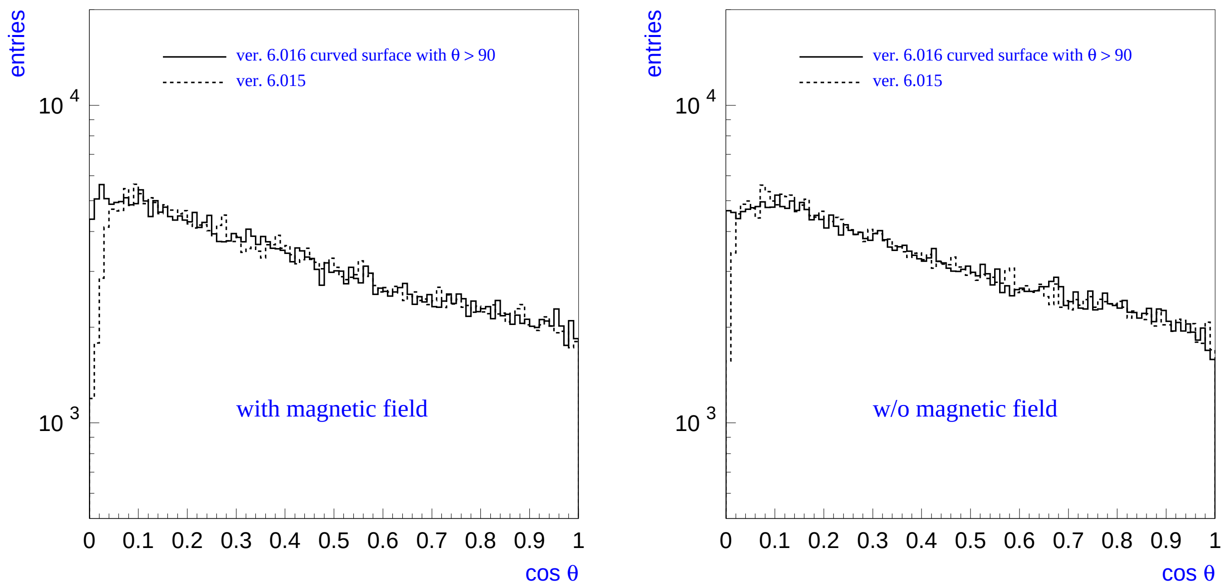

Fig. 6: comparison between previous and current best plots

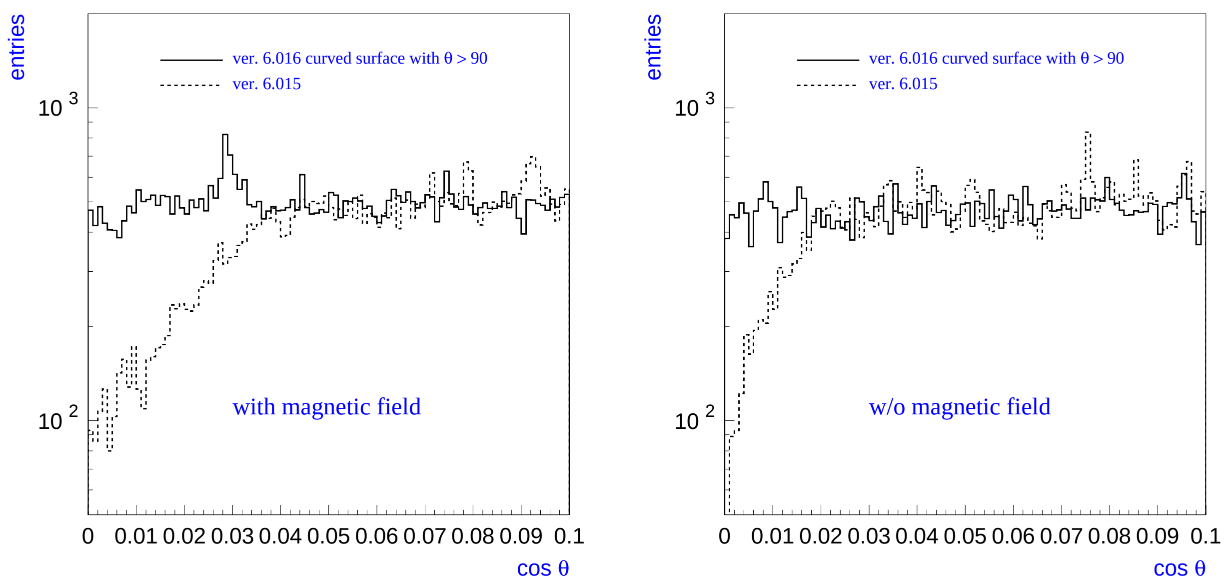

Fig. 7: same as in Fig. 6, magnified in the $0 - 0.1$ $\cos\theta$ range

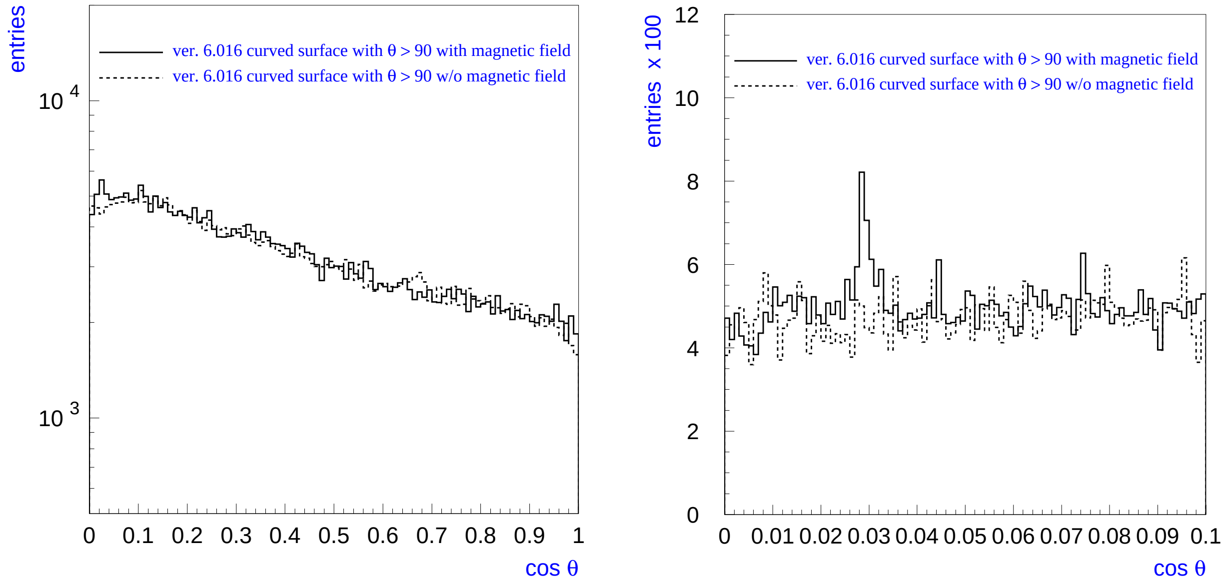

Fig. 8 and 9: comparison of zenith angle distributions with magnetic field on and off

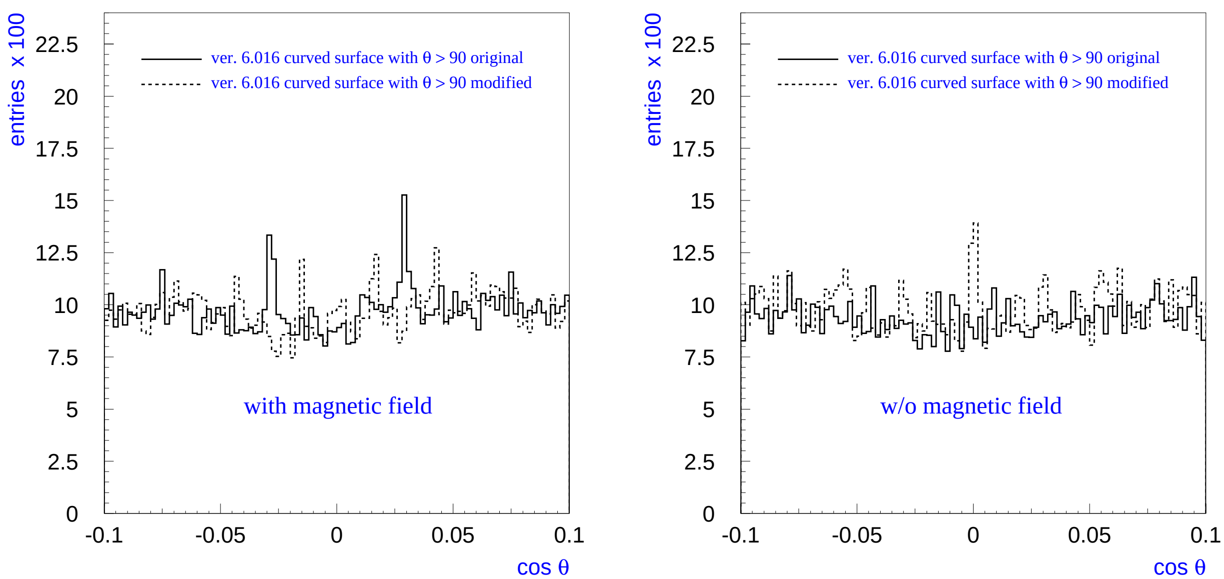

Fig. 10 and 11: comparison of zenith angle distributions with original and modified angle transformation between flat segments

To preserve the correct (isotropic) angular distribution of primaries the zenith angle is first determined by CORSIKA at random in the detector frame (θ_d) and then translated into the internal CORSIKA angle (θ_c). This translation is enabled by the new INPUTS file flag "SCURV T 6.4E8 1.73E5". The shower core location is randomized by "ucr", as usual, which now has a "-curved=[1-4]" flag. The important difference with the flat version is that the previously done curved randomization can no longer be removed. Therefore randomization is no longer performed by the "handle.sh" script. To apply curved randomization, run "ucr" with the following flags: "-LENGTH=[l] -RADIUS=[r] -HEIGHT=2834 -EARTHR=6.4e6 -DEPTH=[1730 or 1695] -curved=4 -cutth=85". Make sure the ratio l/r corresponds to the ratio $l/d = l/2r$ specified by the flag DETCFG in the INPUTS file.

Fig. 4 demonstrates further improvement in the zenith angle distribution gained from application of the coordinate transformation discussed above. Some muons are still missing in the lowest $\cos(\theta)$ bins. These bins can the filled up by including primaries with $\theta > 90$ into the analysis (Fig. 5). Some of these upgoing primaries have created a number of downgoing muons through scattering or by being deflected in the magnetic field.

Since the same angle θ_c can translate into two different angles θ_d, it is possible to generate upgoing flux at the shower core randomization stage (by "ucr") from the same CORSIKA files as downgoing. Options "-curved=4 -cutth=[θ_{cut}]" allow to oversample (x2 on top of the existing oversampling number set by "-over=[number]") events originating from primaries with zenith angles $\theta_{cut} \leq \theta \leq 90$ in the detector frame. This allows one to generate reliable results with only a little bigger Monte Carlo files (and almost no increase in execution time, since "ucr" is extremely fast).

Fig. 6 and 7 demonstrate the comparison of the current angular distribution with the previous, generated with CORSIKA version 6.015. The increase of the entries in angular bins is slowed down as $\cos\theta$ goes to zero, quite to be expected as explained in the introduction. However, the previously present unphysical sharp suppression at zero is completely gone.

Fig. 7 shows a statistically significant deviation from the local mean in the distribution with the magnetic field on at $\cos\theta = 0.028$. It is also visible on Fig. 8, where the curve with the magnetic field is compared to the one without. Therefore it is important to turn the magnetic field on in the simulation. As seen on Fig. 9, this excess is not uniformly distributed over the small $\cos\theta$, but rather is concentrated in one or more peaks. These peaks are likely to be due to the division of the track into locally flat steps performed during the curved atmosphere treatment in CORSIKA. Once the particle moves from one segment to the other, the local density is allowed to jump (by no more than 0.5 g/cm^2), which may cause the peaking structure. Another reason could be the use of an approximation in angle transformations from one segment to the next. Azimuth angles are unchanged and zenith angles are increased by amount of segment rotation. Precise transformations were implemented in a private CORSIKA version (changes available upon request) and angular distributions replotted. Fig. 10 and 11 demonstrate changes in the distributions: the peaks have shifted, which implies that they are unphysical. Although the size of the peaks has decreased, they seem to follow a rather regular pattern, probably from the flat segment approximation in the curved atmosphere treatment, as mentioned above.

Finally, in Fig. 12 the muon zenith angle distribution is shown for angles from 0° to 180°. The distribution looks somewhat mirrored (around $\cos\theta = 0$) because it was produced with "-curved=4 -cutth=0" options, which use each event twice: once as downgoing and once as upgoing.

Fig. 13 $-$ 16 demonstrate the effect of the magnetic field influence on the deviation of muons from the direction of the primary (here called scattering). At zenith angles close to 90° such "magnetic" scattering is particularly strong. Therefore, a large number of upgoing primaries can produce

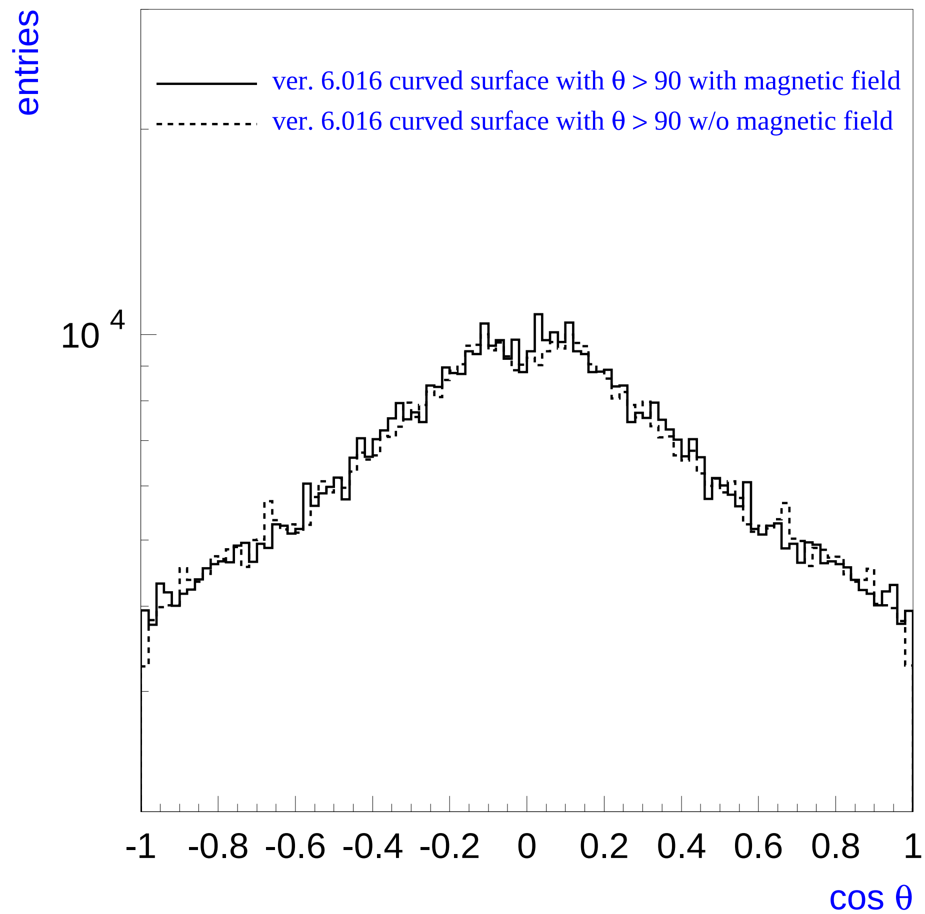

Fig. 12: muon zenith angle distribution from 0° to 180°

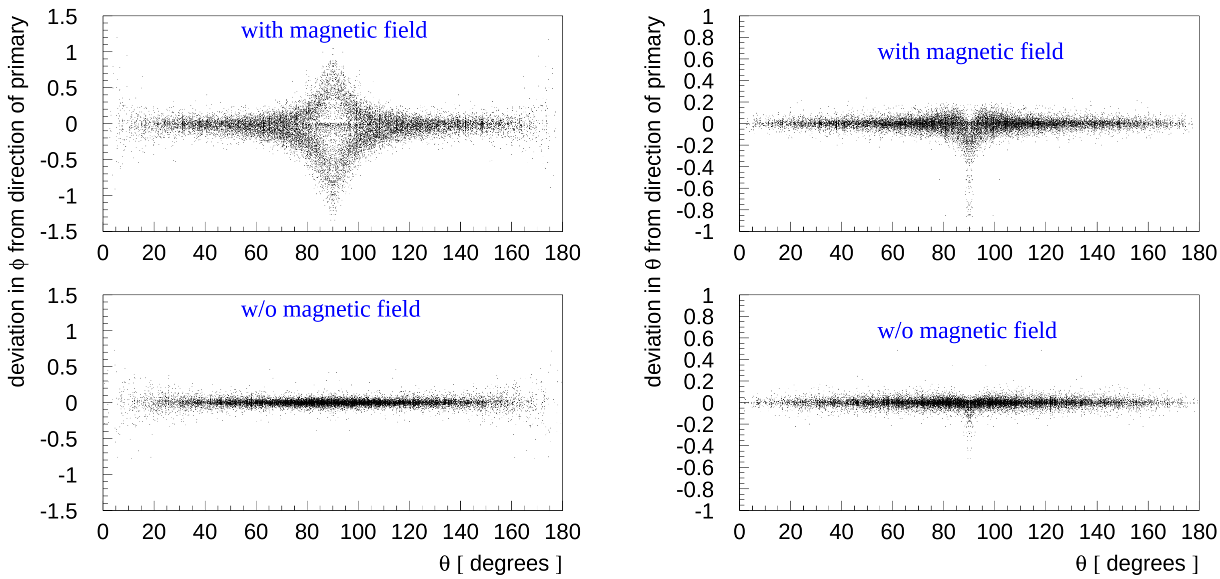

Fig. 13 and 14: deviation of secondaries from primaries

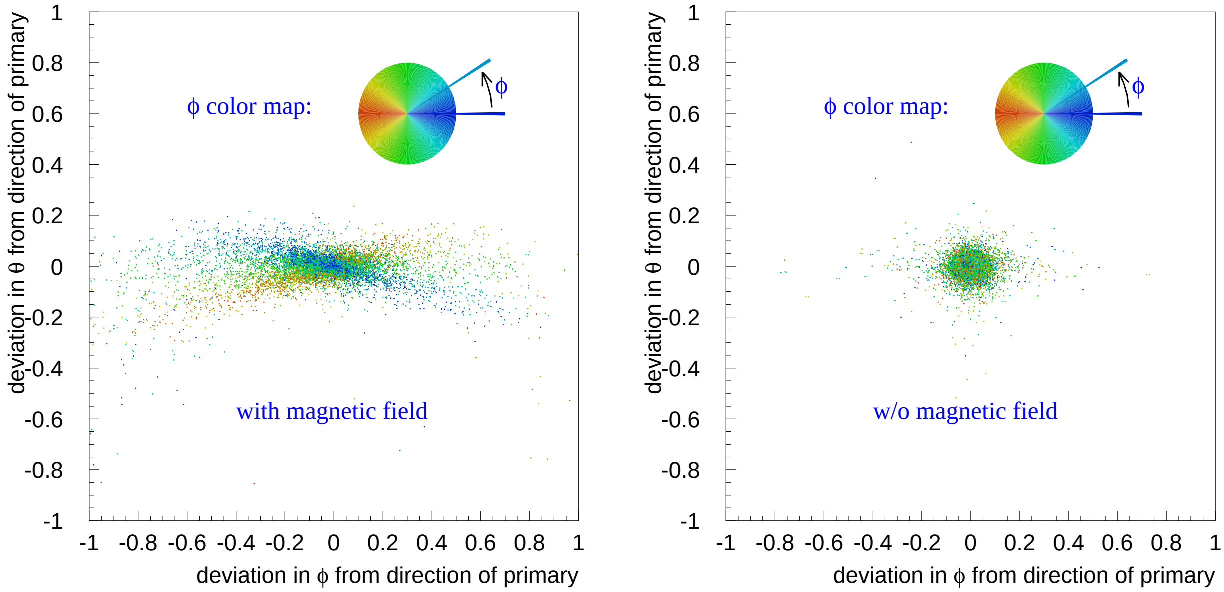

Fig. 15: deviation of secondaries from primaries $\delta\theta$ vs. $\delta\phi$, ϕ color map

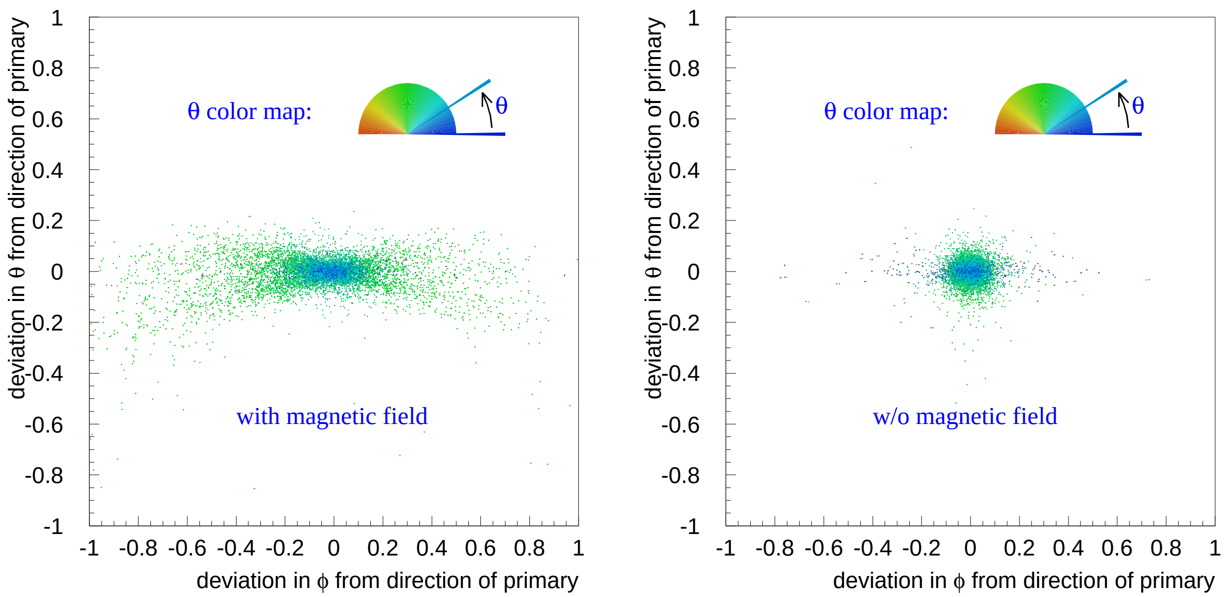

Fig. 16: deviation of secondaries from primaries $\delta\theta$ vs. $\delta\phi$, θ color map

downgoing secondaries. This can be accounted for by generating a few degrees worth of upgoing primaries at just below the horizon, as seen on Fig. 5. In the above discussion up- and down- going primaries are meant in the detector frame, i.e. at least $1.3°$ below the value at which CORSIKA cuts away particles ($90°$). Apparently a small number of particles visible in the detector frame is still lost, as seen on Fig. 14, which shows a small excess of negative over positive $\delta\theta$ deviations of muons from directions of primaries. This excess is exacerbated by the presence of the magnetic field, which adds significantly to the particle scattering.

3 Optimization of dCORSIKA settings

dCORSIKA allows the user to filter out events in which the primary is thought to have an insufficient energy to produce a muon that would reach the detector. This feature saves computational time and disk space and is enabled by the "LOCUT T" flag in the INPUTS file. It is also possible to delete muons (and whole events containing only such muons) that are in the CORSIKA output but cannot reach the detector. This mainly saves disk space and can be done at the "ucr" stage with the "-cutfe=[E_{low}]" flag.

The energy of a muon is compared to the function $E_{cut}(x)$ of the ice thickness x that the muon would have to cross to reach a certain depth h. During the CORSIKA step the energy of the muon for such comparison is assumed to be greater than some fraction ν of the energy of the primary. The depth h is determined from the condition $E_{cut}(h) = E_{low}$, where E_{low} is the energy below which muons are not recorded by CORSIKA (specified by "ECUTS [E_{low}] ..." flag in the INPUTS file) or the value of the "-cutfe=[E_{low}]" flag used by "ucr" (usually also taken as the first argument of the "ECUTS" flag in the corresponding INPUTS file).

The slant depth x is determined as $h/\cos(\theta)$ where θ is the zenith angle of the particle (muon or primary) in the CORSIKA frame of reference. This is a good value even when the surface of the Earth is considered curved as it consistently filters out particles that cannot reach spherical subsurface located at the depth h below the Earth's surface.

To determine the function $E_{cut}(x)$ MMC was run for ice media, muon energies from 105 MeV to 10^{20} eV. For each energy 10^5 muons were propagated to the point of their disappearance and the distance traveled was histogrammed (Fig. 17). This is similar to the analysis done in [2]. However, instead of the average distance traveled, the distance at which only a fraction of muons survives was determined for each muon energy (Fig. 18). Two fixed fractions were selected as candidates: 99% and 99.9%. MMC was run with 2 different settings: $v_{cut} = 10^{-2}$ with the "cont" (continuous randomization feature described in [2]) option and $v_{cut} = 10^{-3}$ without "cont". In Fig. 19 the ratio of distances determined with both settings is displayed for 99% of surviving muons (red line) and for 99.9% (green line). Both lines are very close to 1.0 in most of the energy range except the very low energy part (below 2 GeV) where the muon does not suffer enough interactions with the $v_{cut} = 10^{-2}$ setting before stopping (which means v_{cut} has to be lowered for reliable estimation of the shape of the travelled distance histogram). The ratio of 99% distance to 99.9% distance is also plotted (dark and light blue lines). This ratio is within 10% of 1, i.e. 0.1% of muons travel less than 10% farther than 1% of muons.

$v_{cut} = 10^{-3}$ with no "cont" setting used to determine the maximum range of the 99.9% of the muons was chosen for the estimate of the function $E_{cut}(x)$. In Fig. 20 the χ^2 of the fit is plotted as function of the lower (green) and upper (blue) boundaries of the fit. Using the same argument as in [2] the lower limit is chosen at just below 1 GeV while the upper limit was left at 10^{11} GeV. As seen from the plot, raising the lower boundary to as high as 400 GeV would not lower the χ^2 of the

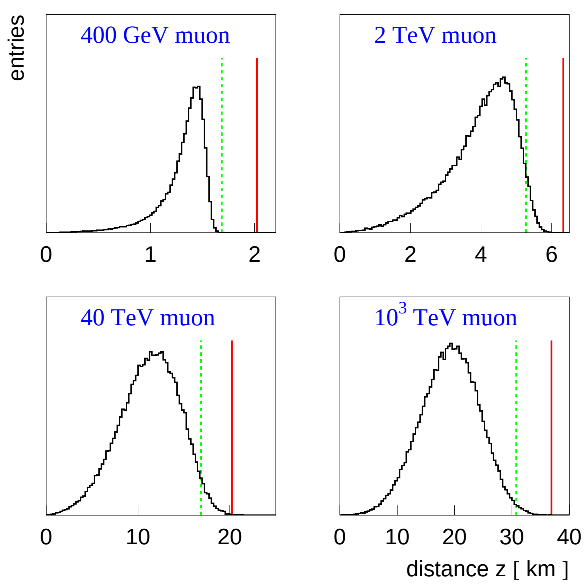

Fig. 17: muon range distributions

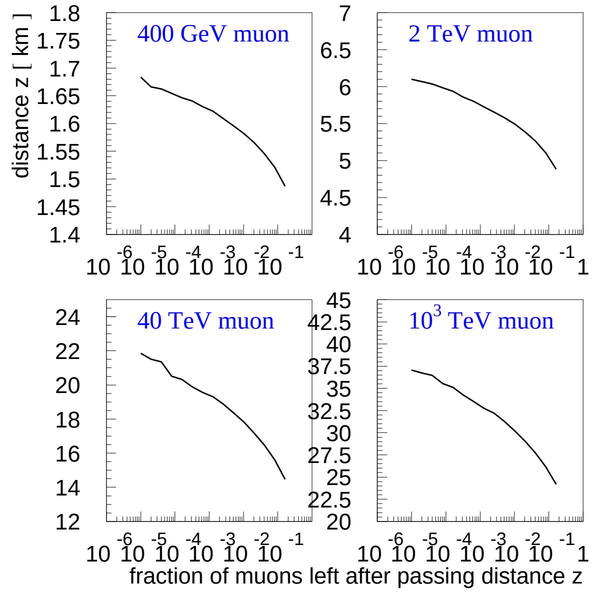

Fig. 18: distance vs. fraction of survived muons

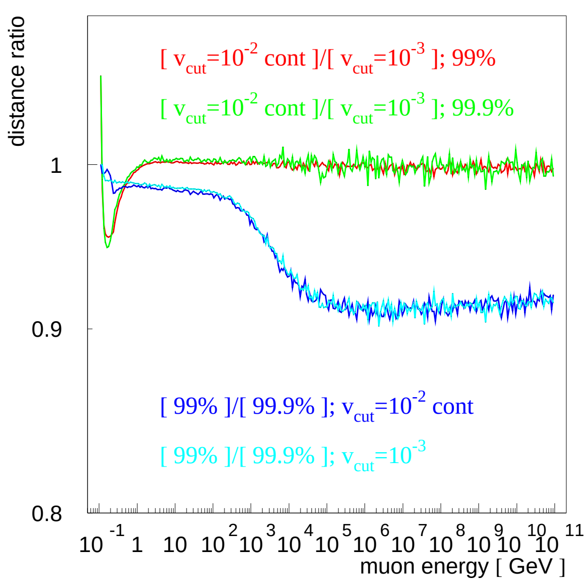

Fig. 19: comparison between different surviving fraction and MMC configuration settings

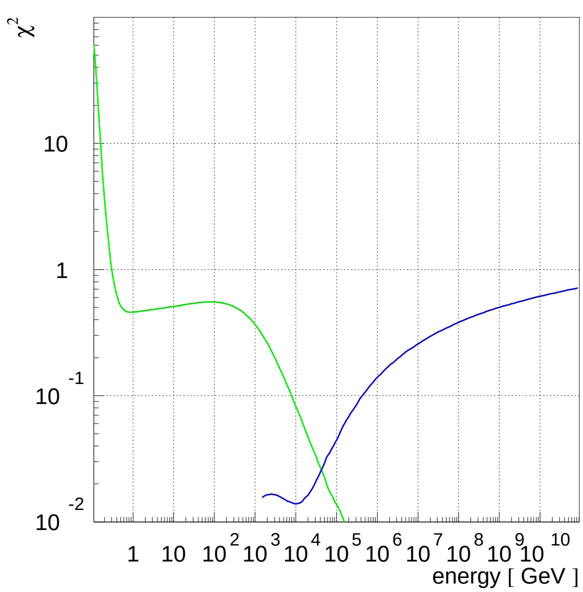

Fig. 20: χ^2 of the fit as a function of fit boundaries

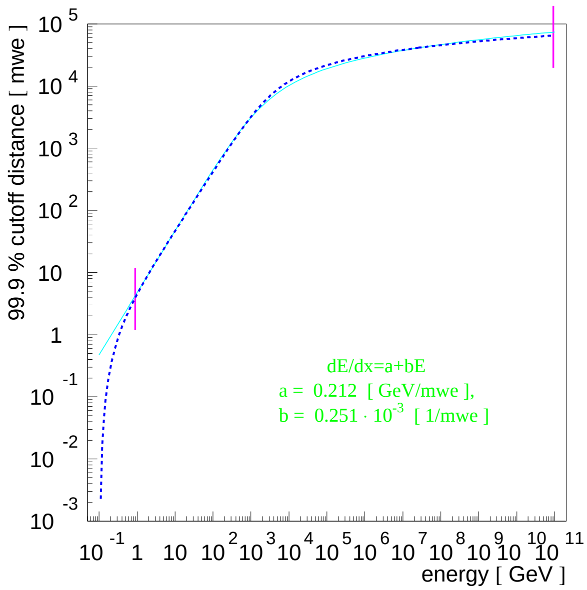

Fig. 21: fit to the $E_{cut}(x)$

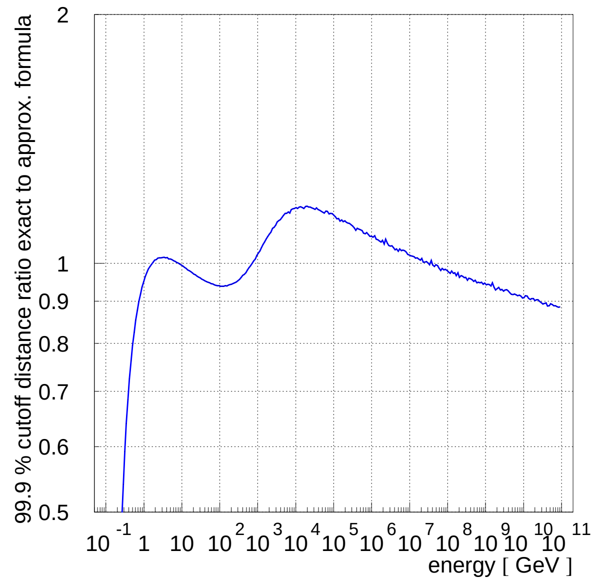

Fig. 22: deviation of the $E_{cut}(x)$ from the fit

fit (and the root mean square of the deviation from it), so the lower boundary was left at 1 GeV for generality of the result. The function fit is

$$x_f = \log(1 + E_i \cdot b/a)/b$$

which is a solution to the equation represented by the usual approximation to the energy losses: $dE/dx = a + bE$. The fit is displayed in Fig. 21 and the deviation of the actual x_f from the fit is shown on Fig. 22. The maximum deviation is less than 20%, which can be accounted for by lowering a and b by 20%. Therefore, the final values used in CORSIKA and "ucr" for the function

$$E_{cut}(x) = (e^{bx} - 1)a/b$$

$$\text{are} \quad a = 0.212/1.2\,\frac{\text{GeV}}{\text{mwe}} \quad \text{and} \quad b = 0.251 \cdot 10^{-3}/1.2\,\frac{1}{\text{mwe}}\,.$$

The distances obtained with these values for 4 different muon energies are shown by red solid lines in Fig. 17. The distances obtained with values of a and b not containing the 1.2 correction factor are shown with green dashed lines.

To determine the fraction ν of the low energy threshold of primaries ($E_{low,pri}$) above which 99% or 99.9% of generated muons are recorded (Fig. 24), more than 10^6 showers with the usual AMANDA settings (spectral indices and weight distribution of primaries, South Pole atmosphere, magnetic field, and elevation, etc.; the angle-dependent cuts described above were disabled) were generated for $E_{low,pri} = E_{low,\mu}$ from 1 GeV to 10^{11} GeV. The actual number of produced muons is shown on Fig. 23 by black dashed line (scale to the right of the plot). The same number normalized to 10^6 showers is shown in red. The fractions $\nu(99\%)$ and $\nu(99.9\%)$ are shown by green-dotted and blue-solid lines respectively (for $E_{low,pri}$ above which less than 100 muons were generated, the energy of the second lowest energy muon is used to determine the 99% fraction, same for $E_{low,pri}$ above

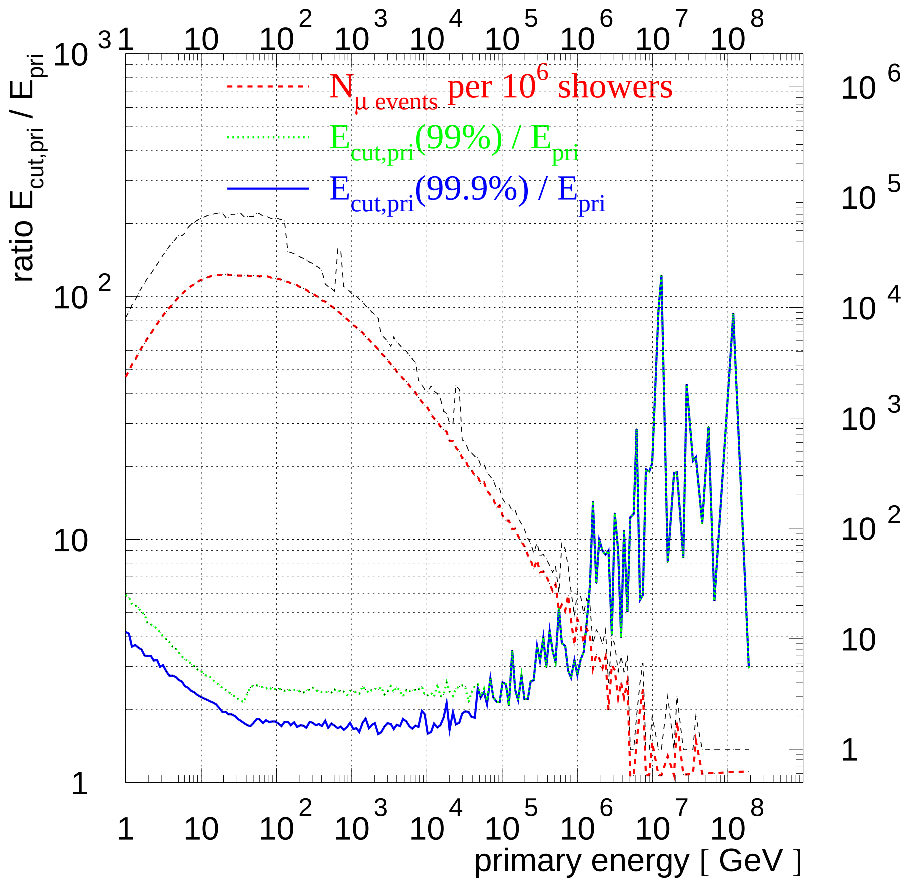

Fig. 23: ratio of the primary to the highest muon energies

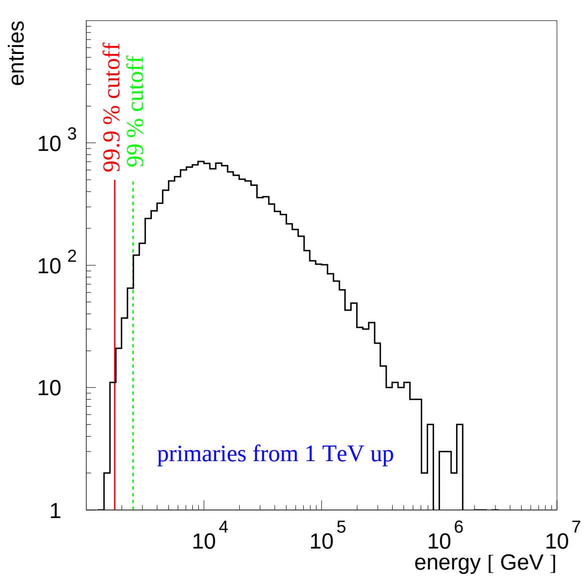

Fig. 24: Distribution of primaries that produce muons with energies higher than 1 TeV

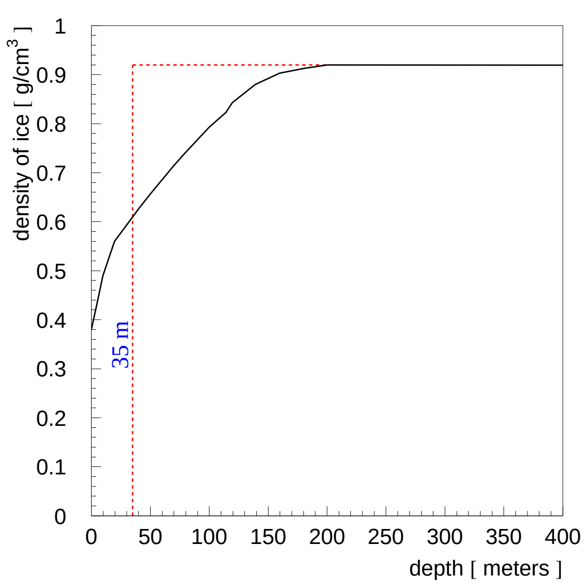

Fig. 25: Ice density profi le correction

which less than 1000 muons were generated, used to determine the 99.9% fraction). The lowest ratios recorded are:

$$\nu_{cut}(99\%) = 2.06 \quad \text{and} \quad \nu_{cut}(99.9\%) = 1.58.$$

These ratios should be used to determine the value of the first argument to "ERANGE" in the INPUTS file once the muon low energy cutoff has been set by the first argument to the "ECUTS" flag.

4 Density depth correction

Paolo [4] suggested that due to the smaller density of ice packed with air bubbles in the first 200 meters under the surface, muons lose less energy while propagating down than with the constant ice density depth profile. To correctly account for that, the exact density profile (Fig. 25) is replaced with the constant density profile starting 35 meters below the actual surface of ice (represented in Fig. 25 by red dashed lines) so that the area under both the actual and artificial profiles is the same. Therefore, instead of 1730 m, 1730-35=1695 m are subtracted from z when going from the CORSIKA to AMANDA coordinates. This value (1695) has to be supplied at the "ucr" step with the "-DEPTH=1695" flag to ensure that shifted by xy (or curved) randomization showers still go through the detector volume.

The muon cross sections in medium are mostly proportional to the density times traveled distance (i.e. mass overburden) with two exceptions. Firstly, the density correction and dielectric suppression effects depend on density weakly and are themselves generally very small (below 1%). Secondly, decay probability is proportional to the distance only (not mass overburden), but is quite small for the interesting muons traveling through 35 m/$\cos(\theta)$ of ice, because these muons still have about 1.5 km/$\cos(\theta)$ of ice to travel through to reach the detector, i.e. they must have quite high energy, thus suppressing the decay probability (which is inversly proportional to energy). Neglecting these effects, the muon traveling through 200 m thick ice layer with real density profile is equivalent to the muon traveling through 165 m thick artificial ice layer with constant density profile.

In the above argument the surface of ice was assumed flat in the CORSIKA coordinate system. This is a good approximation, because the muon traveling through $h = 35$ m of ice at the maximum in the CORSIKA frame angle of $\theta_{max} = 88.67°$ goes only $\delta x = h\tan(\theta) = 1.5$ km away from the point where it enters the ice, and deviation of the surface of ice from flat at that distance is only $R(\cos(\alpha) - 1) \approx R\alpha^2/2 = \delta x^2/2R = 18$ cm.

5 Conclusions

Taking for the density-corrected AMANDA depth a value of $h = 1695$ m, ice density $\rho = 0.917$ g/cm^3, effective dimensions of AMANDA usually used being $r = 400$ m and $l = 800$ m, we get for the muon low energy cutoff $E_{low} = E_{cut}(\rho \cdot (h - l/2)) = E_{cut}(1188\text{ m}) = 238$ GeV. Corresponding value of the low energy cut on the primaries is 490 GeV for 99% of muons recorded and 376 GeV for 99.9% of muons recorded. If instead of the dimensions of the effective detector cylinder the z-coordinate of the highest OMs in B10 of 231.5 m is used (also ususally used to estimate geometrical dimensions of AMANDA-II), one gets $E_{low} = E_{cut}(1342\text{ m}) = 273$ GeV for muons and 563 GeV (99%) or 432 GeV (99.9%) for primaries. It could be possible to further raise these numbers if the lowest energy of muons at which they emit light that can be recorded by the detector were known.

For the calculation above it is assumed to be close to the rest mass of the muon, since for the muon to emit cherenkov light its energy can be as low as $\gtrsim$ 160 MeV. To summarize, the suggested energy cuts are presented in the table:

400 m above the detector center		
fraction	E_{low} for muons	E_{low} for primaries
99%	238 GeV	490 GeV
99.9%	238 GeV	376 GeV

231.5 m above the detector center		
fraction	E_{low} for muons	E_{low} for primaries
99%	273 GeV	563 GeV
99.9%	273 GeV	432 GeV

Execution time and file size (for 10^5 primaries on a 850 MHz P3 computer) are summarized in the following table:

settings	LOCUT F	LOCUT T
time	55 min	18 min
size	131 Kb	97 Kb
size (only muons)	113 Kb	84 Kb
after "ucr" with "-cutfe=[E_{low}]"		
size	42 Kb	42 Kb
size (only muons)	24 Kb	24 Kb

A run with 10^5 primaries with $E_{low,pri} = 376$ GeV corresponds to 0.0266 seconds of detector lifetime with dimensions $l = 800$ m and $r = 400$ m. Using the angle-dependent energy cut for primaries accelerates the program 3 times. If additionally the option "-cutfe=[E_{low}]" is used with "ucr", and only primaries and muons are saved, only 20% of disk space is used compared to the run with no such cuts. Setting the primary cutoff to $E_{low} = 563$ GeV increases the lifetime of the above run to 0.0527 seconds (with no change in execution time).

With the previously used settings ($E_{low,pri} = 800$ GeV, $E_{low,\mu} = 400$ GeV) the corresponding lifetime is 0.0954 seconds. These settings correspond to about 99% of muon producing primaries recorded and 0.1% of lowest energy muons penetrating as deep as $+46$ to -291 m in the detector coordinates (with the previously used $h = 1730$ m depth setting). This report recommends reducing the primary low energy cutoff to at least 563 GeV and the corresponding muon low energy cutoff to 273 GeV.

References

[1] My presentation for AMANDA meeting, 19 September, 2000, Irvine, available here: http://area51.berkeley.edu/~dima/work/

[2] Muon Monte Carlo: a new high-precision tool for muon propagation through matter, ICRC 2001; updated results here: http://area51.berkeley.edu/~dima/work/

[3] CORSIKA history file, the official distribution is here: http://www-ik3.fzk.de/~heck/corsika/

[4] Paolo Desiati, data provided by Buford Price.